

Closed-form solutions for the Lévy-stable distribution

Karina Arias-Calluari,^{1,*} Fernando Alonso-Marroquin,^{1,2} and Michael S. Harré³

¹*School of Civil Engineering, The University of Sydney, Sydney NSW 2006, Australia*

²*Computational Physics IfB, ETH Zurich, CH-8093 Zurich, Switzerland*

³*Complex Systems Research Group, The University of Sydney, Sydney NSW 2006, Australia*



(Received 13 December 2017; revised manuscript received 30 April 2018; published 3 July 2018)

The Lévy-stable distribution is the attractor of distributions which hold power laws with infinite variance. This distribution has been used in a variety of research areas; for example, in economics it is used to model financial market fluctuations and in statistical mechanics it is used as a numerical solution of fractional kinetic equations of anomalous transport. This function does not have an explicit expression and no uniform solution has been proposed yet. This paper presents a uniform analytical approximation for the Lévy-stable distribution based on matching power series expansions. For this solution, the trans-stable function is defined as an auxiliary function which removes the numerical issues of the calculations of the Lévy-stable distribution. Then, the uniform solution is proposed as a result of an asymptotic matching between two types of approximations called “the inner solution” and “the outer solution.” Finally, the results of analytical approximation are compared to the numerical results of the Lévy-stable distribution function, making this uniform solution valid to be applied as an analytical approximation.

DOI: [10.1103/PhysRevE.98.012103](https://doi.org/10.1103/PhysRevE.98.012103)

I. INTRODUCTION

A wide range of natural and social phenomena exhibit a power law in the probability distribution of large events. These tails are characterized by the asymptotic relation $f(x) \sim 1/x^{1+\alpha}$, where x is the size of the events [1,2]. For $0 < \alpha \leq 1$, the distribution has an indefinite mean value. On the other hand, for $1 < \alpha \leq 2$, the distribution has a defined mean value but still exhibits infinite variance [3]. These heavy-tailed distributions have been observed in economics and statistical mechanics.

In the field of economics, the statistics of price returns, trade size, and share volumes have been investigated. Heavy-tailed distributions have been observed in the correlations of the absolute value of the S&P 500 returns [4,5], the effects of networks on price returns [6], daily returns of the Dow Jones index [7], Brent crude oil returns [8], and the aggregate output growth rate distribution [9]. Even after applying five different estimation techniques, power-law tails with the characteristic index α were found on the cumulative distribution of trade size and share volumes of 252 U.S. stocks over the 42-year period from 1963 to 2005 [10,11]. To capture heavy tails different models have been proposed to simulate the stock price dynamics. For instance, models of anomalous diffusion of option pricing were introduced as an extension of the well-known Brownian model [12,13]. These models are focused on different aspects such as capturing the dynamic of the price with waiting times (periods of stagnation) which are Lévy-stable distributed [12] or on the effect of “particles” representing an agent’s interaction [13]. The continuous counterpart of these discrete models is the Fokker-Planck equation (FPE) that is presented in terms of

fractional derivatives. The solution of the FPE gives the time evolution of the probability density function (pdf) of price return [12–14].

In the field of statistical mechanics, the diffusion equation (DE) is a fundamental equation of transport dynamics used to describe a particle motion resulting from the interaction with a thermal heat bath [15–17]. The DE defines the probability of a particle to be at a certain position at a specific time, and its pdf is given by the Gaussian distribution [18–20]. On the other hand, for the generalization of anomalous transport, a fractional diffusion equation (FDE) is used to describe a continuous time random walk model [16,21]. This model generalizes the Brownian diffusion motion based on two parameters accounting for the jump length and the waiting time between two successive jumps. A long-tailed waiting time pdf—long rests—produces a “subdiffusion process” [16,17]. On the opposite case, the Lévy-stable distribution for the jump length pdf—long jumps—produces a “superdiffusion process” [16,22]. The anomalous diffusion under an external velocity field or a microscopic advection is studied by fractional diffusion-advection equations (FDAEs) [16,17,23]. Additionally, the fractional Fokker-Planck equation (FFPE) is used to study the anomalous diffusion under the influence of an external field: electrical bias field [16,17], periodic potentials [24,25], or a harmonic potential [18,21,26]. The FFPE can be derived either from the generalized FDE of continuous time random walk models or from a Langevin equation with Lévy-stable noise or Gaussian noise and long rests [18,25,27,28].

The previous fractional kinetic equations (FDE, FDAE, and FFPE) can be solved in terms of Lévy-stable distribution function that has an analytical solution for only two cases—the normal and Cauchy distributions [29]. In the remaining cases there is not a closed-form expression. Typically the numerical solution of the Lévy-stable distribution has numerical

*kari0293@uni.sydney.edu.au

oscillations in the tail of the distribution. For some cases it displays apparent discontinuity in logarithmic plots because of negative values obtained from the numerical solution [30]. Consequently numerical solutions of the Lévy-stable distribution are not reliable as the probability density function must be positive.

Analytical expressions in terms of power series have been presented by different authors. Feller [31], Montroll and Bendler [32], and Zolotarev [33] used power series to obtain converging algorithms of the Lévy-stable distribution function in two ranges, the first for $\alpha < 1$ and the second for $\alpha > 1$ for symmetric distributions. However, some of the proposed series do not converge to the Lévy-stable function, and some of them are only applicable for extreme values $x \rightarrow 0$ or ∞ . Mantegna [34] presented a solution similar to that of Montroll and Bendler [32] but the algorithm is only valid when $x \rightarrow \infty$ and $0.75 < \alpha \leq 1.95$. Nolan [35] presented an algorithm for asymmetric distributions of large events $x \rightarrow \infty$ focusing only on the tail behavior of the distribution. Thus, the Lévy-stable distribution function does not have an explicit expression [36,37] and no uniform solution of the Lévy-stable distribution has been proposed [31,33,35].

Due to the absence of an explicit expression, numerical solutions were developed to evaluate the Lévy-stable distribution function by using numerical recursive quadrature methods [38–40]. Nolan [38,41] develops a numerical solution for the estimation of Lévy-stable parameters through a maximum likelihood method for each data set of x . However, Nolan’s method converges only for $\alpha > 0.4$ and the convergence to the Lévy-stable distribution function seems to be not accurate enough. Despite this fact, Nolan’s method constitutes an important method that is still being used [39].

Apart from the numerical issues in the evaluation of the Lévy-stable distribution, some authors have pointed out its infinite variance as a drawback [42–44]. To avoid the infinite variance of the Lévy-stable distribution function, several truncations are proposed. The truncation was justified by the observed change of slope of the tails on extensive datasets [45]. For example, when evaluating the returns per minute of S&P 500 index data over the ten-year period from 1985 to 1995 a change of slope from $\alpha = 1.4$ to 3 was found. The truncations make the variance finite, consequently the distribution function of the sum of independent random variables converges to the normal distribution due to the central limit theorem for large N . Nevertheless, a time series in some stock market indices can exhibit infinite variance; one such case is the variance of price fluctuations in Shanghai stock market index, which increases when the time frame is enlarged [46,47], following a power law with an exponent different from 0.5.

The aim of this paper is to formulate a uniform analytical approximation for the Lévy-stable distribution function based on a series expansion. To achieve this aim we propose several regularizations of the inner and outer series expansions to ensure convergence. This will be an important tool to get the most accurate approximation reducing numerical errors (oscillations) when the Lévy-stable function is evaluated.

This paper is divided in two parts. The first part introduces the Lévy-stable distribution and the trans-stable function. They are defined by Fourier transformations in Secs. III and IV, respectively. The trans-stable function is shown to be identical

to the Lévy-stable distribution for $\alpha < 1$ and it has the same asymptotic behavior for $\alpha > 1$ for large events. The second part refers to Sec. V and it deals with the closed form—analytical approximations—of the Lévy-stable distribution. For this purpose, two types of approximations are developed. The first approximation refers to the inner expansion that converges asymptotically to the Lévy-stable distribution as $x \rightarrow 0$. The second approximation refers to the outer expansion that converges asymptotically as $x \rightarrow \infty$. For the outer expansion two cases are presented; one is obtained from the Lévy-stable function in Sec. VB and the second one is obtained from the trans-stable function in Sec. VC. Finally, the uniform solution in Sec. VI is proposed as a result of matching the inner and the outer solution. The analytical equation of the uniform solution proposed in this paper gives an approximated solution of the Lévy-stable distribution function over the range $-\infty < x < \infty$.

II. CENTRAL LIMIT THEOREM FOR LÉVY-STABLE FLIGHTS

Section 35 of the book by Gnedenko and Kolmogorov [48] shows that the normal distribution is an “attractor” of distributions with finite variances. On the other hand, the attractor of power-law distributions with infinite variances corresponds to the more general “Lévy-stable law.” In other words the Lévy-stable distribution is a specific function to which other distributions converge.

The fundamental concept of attractors is formulated as follows. If a normalized sum of a set of independent, identically distributed random variables $\{X_1, X_2, X_3, \dots, X_N\}$ satisfies

$$\lim_{N \rightarrow \infty} \frac{1}{\sigma_N} \left(\sum_{i=1}^N X_i - \mu_N \right) = X, \quad (1)$$

then X belongs to the stable law. The coefficients μ_N and σ_N represent the centering and normalizing values, respectively [48].

The Gnedenko-Kolmogorov theorem is a generalization of the classical central limit theorem which states that the normalized sum of independent random variables with finite variance in Eq. (1) converges to a variable that is normally distributed [48,49]. This is the case of distributions with power-law tails ($\alpha \geq 2$) with finite variance. The normalized coefficient is $\sigma_N = \sqrt{N}$ and the centering coefficient is $\mu_N = NE[X]$, where N represents the length of the sum and $E[X]$ refers to expected value [50,51]. On the other hand, for independent random variables which hold power-law distributions with infinite variances¹ $0 < \alpha < 2$, Zolotarev [33] and Uchaikin and Zolotarev [51] show that X in Eq. (1) follows a symmetric Lévy-stable law if the normalization coefficient is $\sigma_N = N^{1/\alpha}$ and the centering coefficient is $\mu_N = 0$ for $\alpha \leq 1$ or $\mu_N = NE[X]$ for $\alpha > 1$.

Lévy-stable distributions belong to a wider class of infinitely divisible (ID) distributions. A random variable X is ID

¹Infinite variance is observed for $0 < \alpha < 2$. This characteristic occurs for $0 < \alpha \leq 1$, as a consequence of not having a well-defined expected value $E[X]$. For $1 < \alpha < 2$, the integral in the variance definition diverges [31,33,51].

if it can be represented as the sum of a number N of independent and identically distributed random variables with a common law (N) [52], i.e.,

$$X = \sum_{i=1}^N Y_i^{(N)} \quad \forall N \in \mathbb{N}. \quad (2)$$

The pdf of X is $f(x)$. If $f(x)$ is Lévy stable, then $f(x)$ is an ID distribution function. The proof of this statement is obtained by replacing $Y_i^{(N)} = (X_i - \mu_N)/\sigma_N$ in Eq. (2). Then, by applying the limit $N \rightarrow \infty$ Eq. (1) is obtained. An equivalent definition of infinite divisibility can be given in terms of the characteristic function. The characteristic function is defined as the Fourier transform of the probability density function $f(x)$:

$$\varphi(t) = \mathbb{E}(e^{itx}) = \int_{-\infty}^{\infty} f(x)e^{itx} dx. \quad (3)$$

The characteristic function of the ID distribution can be derived as follows. Consider X as a sum of two independent random variables $X = Y_1 + Y_2$ with pdf's $f_1(x)$ and $f_2(x)$, respectively. For the convolution of the two probability distributions [44], the pdf of X has the form

$$f(x) = \int_{-\infty}^{\infty} f_1(k)f_2(x-k)dk. \quad (4)$$

By substituting Eq. (4) into Eq. (3) and interchanging the order of the integration the equation for the characteristic function of X is obtained:

$$\varphi_X(t) = \varphi_{Y_1}(t)\varphi_{Y_2}(t). \quad (5)$$

Assuming that Y_1 and Y_2 are identically distributed, the characteristic function of $f(x)$ can be defined as $\varphi_X(t, 2) = [\varphi(t)]^2$. In general, for the sum of N independent and identically distributed random variables in Eq. (2), the characteristic function is given by

$$\varphi_X(t, N) = [\varphi_N(t)]^N. \quad (6)$$

Consequently, Eqs. (2) and (6) are equivalent. Then, the limit is applied in Eq. (6), $\varphi_X(t) = \lim_{N \rightarrow \infty} \varphi_X(t, N)$. As a consequence, $\varphi_X(t)$ is the characteristic function of the pdf of the random variable X . This statement constitutes the Levy continuity theorem that guarantees pointwise convergence [52,53]. The Lévy-Khintchine formula or triple Lévy gives the general equation for ID distributions [52]. This formula determines the class of characteristic function where the pdf is calculated from its Fourier transform [53–56]. The Lévy-stable distribution constitutes a special case of the general Lévy-Khintchine formula in the one-dimensional case that is presented in the next section [53].

III. LÉVY-STABLE DISTRIBUTION FUNCTION

The Lévy-stable distribution is given by the Fourier transform of Eq. (3):

$$f(x; \alpha, \beta, \sigma, \mu) = \frac{1}{2\pi} \int_{-\infty}^{\infty} \varphi(t; \alpha, \beta, \sigma, \mu) e^{ixt} dt, \quad (7)$$

where $\varphi(t)$ is presented in Sec. 34 of the Gnedenko-Kolmogorov book [48] as

$$\varphi(t; \alpha, \beta, \sigma, \mu) = e^{i(t\mu - |\sigma t|^\alpha [1 - i\beta \text{sgn}(t)\Phi])}. \quad (8)$$

The four parameters involved are the stability parameter $\alpha \in (0, 2]$, the skewness parameter $\beta \in [-1, 1]$, the scale parameter $\sigma \in (0, +\infty)$, and the location parameter $\mu \in (-\infty, +\infty)$. The parameter α constitutes the characteristic exponent of the asymptotic power law in the tails and it determines whether the mean value and the variance exist. The Lévy-stable distribution with $0 < \alpha \leq 1$ does not have a mean value and it has a well-defined variance only for $\alpha = 2$ [57].

The function $\text{sgn}(t)$ represents the sign of t and the function Φ is defined as

$$\Phi = \begin{cases} \tan\left(\frac{\pi\alpha}{2}\right) & \alpha \neq 1, \\ -\frac{2}{\pi} \log|t| & \alpha = 1. \end{cases} \quad (9)$$

The Lévy-stable distribution is the family of all attractors of normalized sums of independent and identically distributed random variables. The most well-known Lévy-stable distribution functions are the Cauchy distribution with $\alpha = 1$ and the normal distribution function with $\alpha = 2$. Both functions have $\beta = 0$, which means they are symmetric distributions about their mean [33].

In this paper we will focus on symmetric distributions. For this case the Lévy-stable distribution can be normalized as follows:

$$f(x; \alpha, \beta = 0, \sigma, \mu) = \text{Re} \left\{ S \left(\frac{x - \mu}{\sigma}, \alpha \right) \right\}, \quad (10)$$

where the general distribution function is given by the following equation:

$$S(x; \alpha) = \frac{1}{\pi} \int_0^{\infty} e^{-t^\alpha} e^{ixt} dt. \quad (11)$$

The real part of this function corresponds to the normalized Lévy-stable distribution:

$$s(x; \alpha) = \text{Re}[S(x; \alpha)].$$

Consequently, by applying Euler's formula we arrive at [58]

$$s(x; \alpha) = \frac{1}{\pi} \int_0^{\infty} e^{-t^\alpha} \cos(tx) dt. \quad (12)$$

IV. TRANS-STABLE FUNCTION

Zolotarev used the term “trans-stable” to refer to a power series expansion that converges to the Lévy-stable distribution for $0 < \alpha < 1$ only [33]. In this paper, trans-stable is the function that includes a solution that originates a Zolotarev series when the series expansions are applied around $x \rightarrow \infty$. First we define the *complex trans-stable function* in the range of $0 < \alpha < 2$. For $\alpha < 1$, the Lévy-stable distribution and the trans-stable function are identical. For $\alpha > 1$, the trans-stable function and the Lévy-stable distribution present the same asymptotic behavior for $x \rightarrow \infty$. Consequently, our trans-stable function can be used to find a Lévy-stable distribution function for $\alpha > 1$ for large events.

First, the complex trans-stable function is defined as an integral over the path C in the complex plane:

$$G_C(x; \alpha) = \frac{1}{\pi} \int_C I(x, z; \alpha) dz, \quad (13)$$

where

$$I(x, z; \alpha) = e^{-z^\alpha} e^{ixz}. \quad (14)$$

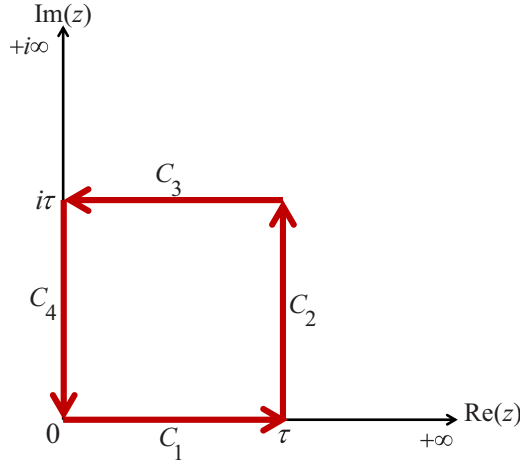


FIG. 1. Contour integration for Eq. (13).

The relation of this function to the Lévy-stable $S(x; \alpha)$ and the trans-stable $T(x; \alpha)$ functions is obtained by choosing a particular path C in the complex plane. Then, the Lévy-stable distribution and trans-stable function are given by Eqs. (15) and (16), respectively:

$$S(x; \alpha) = G_{[0, \infty)}(x; \alpha) = \frac{1}{\pi} \int_0^{\infty} e^{-t^\alpha} e^{ixt} dt, \quad (15)$$

$$T(x; \alpha) = G_{[0, i\infty)}(x; \alpha) = \frac{1}{\pi} \int_0^{i\infty} e^{-t^\alpha} e^{ixt} dt. \quad (16)$$

First it will be shown that for $0 < \alpha \leq 1$ both Lévy-stable $S(x; \alpha)$ and trans-stable $T(x; \alpha)$ functions are identical. For $1 < \alpha < 2$ it will be demonstrated that both functions exhibit the same asymptotic behavior when $x \rightarrow \infty$.

This demonstration is based on the evaluation of the *complex trans-stable integral* Eq. (13) using polar representation for $\alpha \leq 1$ and rectangular representation for $\alpha > 1$ on the complex integrand. The demonstrations are presented in the following subsections.

A. For $0 < \alpha \leq 1$

Here we will show that for $0 < \alpha \leq 1$ the Lévy-stable and trans-stable functions are identical. This demonstration will be done by considering the closed contour shown in Fig. 1. Since the complex function in Eq. (14) is analytical over the complex plane, the integral over the closed contour Eq. (13) is zero:

$$\oint I(x, z; \alpha) dz = 0. \quad (17)$$

Let us take the contour in Fig. 1 that can be divided into four straight paths so that

$$\sum_{i=1}^4 \int_{C_i} I(x, z; \alpha) dz = 0. \quad (18)$$

Now, we will take the limit when $\tau \rightarrow \infty$ in Fig. 1. Using Eqs. (15), (16), and (18) the following equation is obtained:

$$S(x; \alpha) - T(x; \alpha) = -\lim_{\tau \rightarrow \infty} \sum_{i=2}^3 \int_{C_i} I(x, z; \alpha) dz. \quad (19)$$

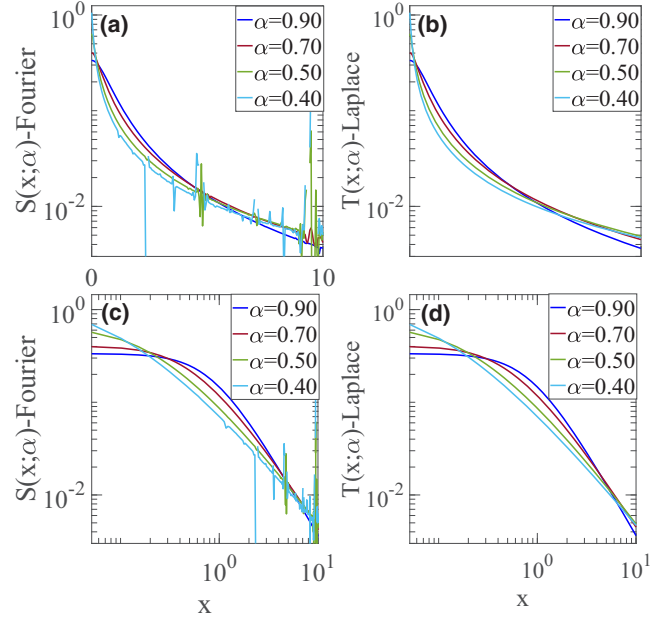


FIG. 2. Comparison of numerical integration $0 < \alpha < 1$ between the Fourier and Laplace transform of the Lévy-stable $S(x; \alpha)$ and the trans-stable $T(x; \alpha)$ functions using recursive adaptive Simpson quadrature method [60]. The absolute error tolerance of the method is $\xi = 3.5 \times 10^{-8}$. The subfigures (a) and (b) are shown in semilogarithmic scale and subfigures (c) and (d) are shown in logarithmic scale.

To evaluate the right hand side in Eq. (19) it is convenient to use the polar representation of the complex number $z = r e^{i\theta}$ and express Eq. (14) in polar coordinates:

$$I(x, z; \alpha) = e^{g(x, r, \theta; \alpha) + ih(x, r, \theta; \alpha)}, \quad (20)$$

$$g(x, r, \theta; \alpha) = -r^\alpha \cos(\theta\alpha) - rx \sin \theta, \quad (21)$$

$$h(x, r, \theta; \alpha) = -r^\alpha \sin(\theta\alpha) + rx \cos \theta. \quad (22)$$

We will adopt the nomenclature of signal theory, where the polar notation separates the effects of instantaneous amplitude $|I| = e^g$ and its instantaneous phase h of a complex function [59]. Consequently, $g(x, r, \theta; \alpha)$ represents the *attenuation factor* and $h(x, r, \theta; \alpha)$ represents the *oscillation factor*.

Now let us notice that $\lim_{r \rightarrow \infty} g(x, r, \theta; \alpha) = -\infty$ for $0 < \alpha \leq 1$ at any value of x . This statement is based on the fact that $\cos(\theta\alpha) \geq 0$ in the first quadrant for $\alpha \leq 1$. Consequently, $\lim_{r \rightarrow \infty} I(x, z; \alpha) = 0$ so that the integral of the right side of Eq. (19) vanishes at $\tau \rightarrow \infty$, therefore

$$S(x; \alpha) = T(x; \alpha) \quad \text{if } 0 < \alpha \leq 1. \quad (23)$$

So, Eq. (23) will allow us to use the trans-stable function $T(x; \alpha)$ instead of the Lévy-stable distribution function $S(x; \alpha)$ for $0 < \alpha \leq 1$ in the numerical integration. This is with the aim to remove numerical oscillation, specifically in the tails. It is noticeable that the integration of the trans-stable function $T(x; \alpha)$ in Eq. (16) is performed over the imaginary axis. Applying the following change of variable $t \rightarrow -it$ (formally done by defining $u = -it$ so that $du = -idt$ and later replacing the dummy variable u by t inside the integral), the

TABLE I. Summary of Fourier and Laplace representations for the Lévy-stable and the trans-stable functions.

	Lévy-stable distribution $S(x; \alpha)$	Trans-stable function $T(x; \alpha)$
Fourier transform	$\frac{1}{\pi} \int_0^\infty e^{-t^\alpha} e^{ixt} dt$	$\frac{1}{\pi} \int_0^{i\infty} e^{-t^\alpha} e^{ixt} dt$
Laplace transform	$\frac{1}{\pi} \int_0^{-i\infty} e^{-(it)^\alpha} e^{-xt} i dt$	$\frac{1}{\pi} \int_0^\infty e^{-(it)^\alpha} e^{-xt} i dt$

trans-stable function is converted into a Laplace transformation. Consequently, the integration is performed over the real axis. The Fourier and Laplace representations for $T(x; \alpha)$ are shown in Eq. (24):

$$T(x; \alpha) = \frac{1}{\pi} \int_0^{i\infty} e^{-t^\alpha} e^{ixt} dt = \frac{1}{\pi} \int_0^\infty e^{-(it)^\alpha} e^{-xt} i dt. \tag{24}$$

Figure 2 compares the Fourier representation of the Lévy-stable distribution function $S(x; \alpha)$ and the Laplace representation of trans-stable function $T(x; \alpha)$. The integration is performed using a recursive adaptive Simpson quadrature method [60]. It is evident that the Laplace representation removes the oscillations of the Fourier representation of the Lévy-stable distribution for $\alpha < 1$.

It is important to add that the Lévy-stable distribution function and trans-stable function hold the same value for their Fourier and Laplace transform representations. The difference between each transform representation is the axis in which each function is integrated. The expressions are shown in Table I.

B. For $1 < \alpha < 2$

Here we will show that for $1 < \alpha < 2$ the Lévy-stable and trans-stable functions have the same asymptotic behavior on large events if the integrals are appropriately truncated.

Let us recall Eq. (21) for the attenuation factor:

$$g(x, r, \theta; \alpha) = -r^\alpha \cos(\theta\alpha) - rx \sin \theta.$$

In the previous section, it was shown that $\cos(\theta\alpha)$ is always positive in the first quadrant of the complex plane if $0 < \alpha \leq 1$. Otherwise, if $\alpha > 1$, then $\cos(\theta\alpha) < 0$ when $\theta = \pi/2$. Consequently, $\lim_{r \rightarrow \infty} I(x, r, \theta; \alpha) = \infty$ in this range, so that the right hand side of Eq. (19) cannot be neglected. Therefore $S(x) \neq T(x)$ if $\alpha > 1$.

We can find an approximation between these two functions if the τ value in the contour of Fig. 1 is kept large but finite ($\tau < \infty$). Thus, Eq. (18) becomes

$$S(x; \alpha, \tau) - T(x; \alpha, \tau) = - \sum_{i=2}^3 \int_{S_i} I(x, z; \alpha) dz, \tag{25}$$

where $S(x; \alpha, \tau)$ and $T(x; \alpha, \tau)$ are the truncated integrals in Eqs. (15) and (16), respectively:

$$S(x; \alpha, \tau) = \frac{1}{\pi} \int_0^\tau e^{-t^\alpha} e^{ixt} dt, \tag{26}$$

$$T(x; \alpha, \tau) = \frac{1}{\pi} \int_0^{i\tau} e^{-t^\alpha} e^{ixt} dt. \tag{27}$$

Now, the right hand of Eq. (25) can be evaluated in the limit where $x \rightarrow \infty$. First, notice that in the contour of integration in Fig. 1 the magnitude of r is bounded by the condition $0 < r < \sqrt{2}\tau$ and $\sin(\theta) > 0$ in the first quadrant, thus

$$\lim_{x \rightarrow \infty} g(x, r, \theta; \alpha) = -\infty.$$

Consequently, $\lim_{x \rightarrow \infty} I(x, z; \alpha) = 0$ so that the integral on the right of Eq. (25) vanishes at $x \rightarrow \infty$. Therefore, the asymptotic behavior is obtained for $1 < \alpha < 2$:

$$S(x; \alpha, \tau) \sim T(x; \alpha, \tau) \text{ as } x \rightarrow \infty. \tag{28}$$

This demonstrates that both functions are asymptotically equivalent when the integrals are truncated.

The next step is to find the truncation value τ that leads to the best approximation of these functions. The value of τ should be chosen to minimize the truncation error and at the same time to make the domain of integration as small as possible. With this aim, the trans-stable function $T(x; \alpha, \tau)$ in Eq. (16) is expressed in its Laplace representation by using the change of variable $t \rightarrow -it$. Thus,

$$T(x; \alpha, \tau) = \frac{1}{\pi} \int_0^\tau \bar{I}(x, t; \alpha) dt, \tag{29}$$

where \bar{I} corresponds to the Laplace transform integrand shown in Eq. (24) and Table I:

$$\bar{I}(x, t; \alpha) = e^{(-it)^\alpha} e^{-xt} i. \tag{30}$$

Then, considering Euler’s representation for a complex exponential function $e^{i\theta} = \cos(\theta) + i\sin(\theta)$, the following equations are obtained to express Eq. (30):

$$\bar{I}(x, t; \alpha) = e^{\bar{g}(x, t; \alpha) + i\bar{h}(x, t; \alpha)}, \tag{31}$$

$$\bar{g}(x, t; \alpha) = -t^\alpha \cos\left(\frac{\pi\alpha}{2}\right) - xt, \tag{32}$$

$$\bar{h}(x, t; \alpha) = -t^\alpha \sin\left(\frac{\pi\alpha}{2}\right) + \frac{\pi}{2}. \tag{33}$$

The instantaneous amplitude $|\bar{I}| = e^{\bar{g}}$ will be determined by the attenuation factor in Eq. (32). For that reason, an analysis of $\bar{g}(x, t; \alpha)$ was made in Fig. 3. The curve $\bar{g}(x, t; \alpha) = 0$ divides two regions, one with exponential growth ($\bar{g} > 0$) and the other with exponential decay ($\bar{g} < 0$).

In Fig. 3, two subregions can be recognized in $\bar{g} < 0$. The first one is “zone A,” which contains negative \bar{g} values with downward trend $\partial\bar{g}/\partial t < 0$ that is faster as $x \rightarrow \infty$. The second subregion is “zone B,” which contains smaller negative \bar{g} values that follow an upward trend and $\partial\bar{g}/\partial t > 0$ displaying an increase behavior when $x \rightarrow 0$. Considering these subregions, the truncation τ in Eq. (29) will depend on the x value as follows.

(1) For $x \rightarrow 0$, the integration must avoid zone B. The values of $\bar{g}(x, t; \alpha)$ in this zone lead to an exponential growth due to an upward trend $\partial\bar{g}/\partial t > 0$, consequently $|\bar{I}| \rightarrow 0$.

(2) For $x \rightarrow \infty$, the integration should be restricted to zone A. The downward trend $\partial\bar{g}/\partial t < 0$ leads us to obtain $\bar{g}(x, t; \alpha) \rightarrow 0$. Consequently, the convergence of $|\bar{I}| \rightarrow 0$ occurs faster as $t \rightarrow \infty$.

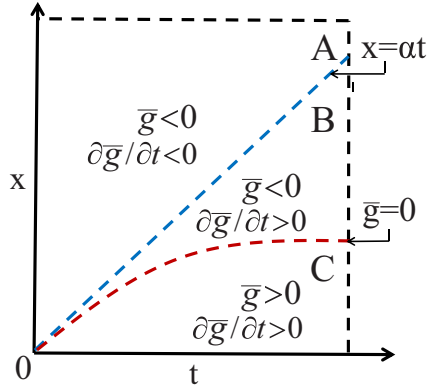


FIG. 3. Curve $\bar{g} = 0$ separates two regions with $\bar{g} > 0$ and $\bar{g} < 0$. In the latter region, two zones can be distinguished: zone A, which contains negative values with downward trend $\partial \bar{g} / \partial t < 0$, and zone B, which contains negative values with upward trend $\partial \bar{g} / \partial t > 0$. The equation $x = \alpha t$ is an estimation of the boundary between zones A and B.

For $x \rightarrow 0$, the cutoff τ_1 which avoids most of zone B is defined by $x = \alpha t$. This equation is an estimation of the boundary between zones A and B for the full range of α values.

The cutoff τ_1 obeys a linear equation and is obtained from the following equations:

$$e^{\bar{g}(x, \tau_1; \alpha)} = |\bar{I}| = \epsilon \quad \text{and} \quad x = \alpha \tau_1, \quad (34)$$

where the tolerance ϵ represents a negligible instantaneous amplitude $|\bar{I}|$.

For $x \rightarrow \infty$, the cutoff τ_1 will restrict the integration of \bar{I} on a closed interval $[0, t_c]$. This occurs due to a faster downward trend $\partial \bar{g} / \partial t < 0$. The t_c value represents the point where the instantaneous amplitude can be considered a negligible quantity $|\bar{I}| = \epsilon$. Thus, the cutoff τ_1 obeys an equation of a vertical line $\tau_1 = t_c$.

Notice that there are two different definitions for τ_1 . Each one corresponds to a particular subregion A ($x \rightarrow \infty$) or B ($x \rightarrow 0$). Consequently, the truncation τ_1 for the trans-stable function is defined by two equations which depend on the x and ϵ values. These two equations have their intersection point at (t_c, x_c) :

$$\tau_1(\epsilon, x) = \begin{cases} t_c(\epsilon) & \text{if } x > x_c \\ x/\alpha & \text{if } x < x_c \end{cases} \quad \text{for } \alpha > 1, \quad (35)$$

where $t_c(\epsilon)$ and x_c are given by the implicit form of the following equations:

$$\alpha t_c^2 + t_c^\alpha \cos(\pi \alpha / 2) + \ln(\epsilon) = 0, \quad (36)$$

$$x_c = \alpha t_c.$$

Figure 4 illustrates the contour plot of the instantaneous amplitude $|\bar{I}|$ for $\alpha = 1.4$. The truncation τ_1 is presented as a cutoff made when a negligible value of instantaneous amplitude is achieved $|\bar{I}| = \epsilon = 10^{-3}$. The point (x_c, t_c) is located at the intersection between the contour line of the given tolerance ϵ and the equation $\tau_1 = x/\alpha$. The truncation τ_1 avoids zone B, which contains negative values for \bar{g} with $\partial \bar{g} / \partial t > 0$. One can observe that there is an abrupt upward trend in $|\bar{I}|$ for $x \rightarrow 0$. So, the truncation τ_1 allows us to make a perfect cutoff before this upward trend starts. It is noticeable

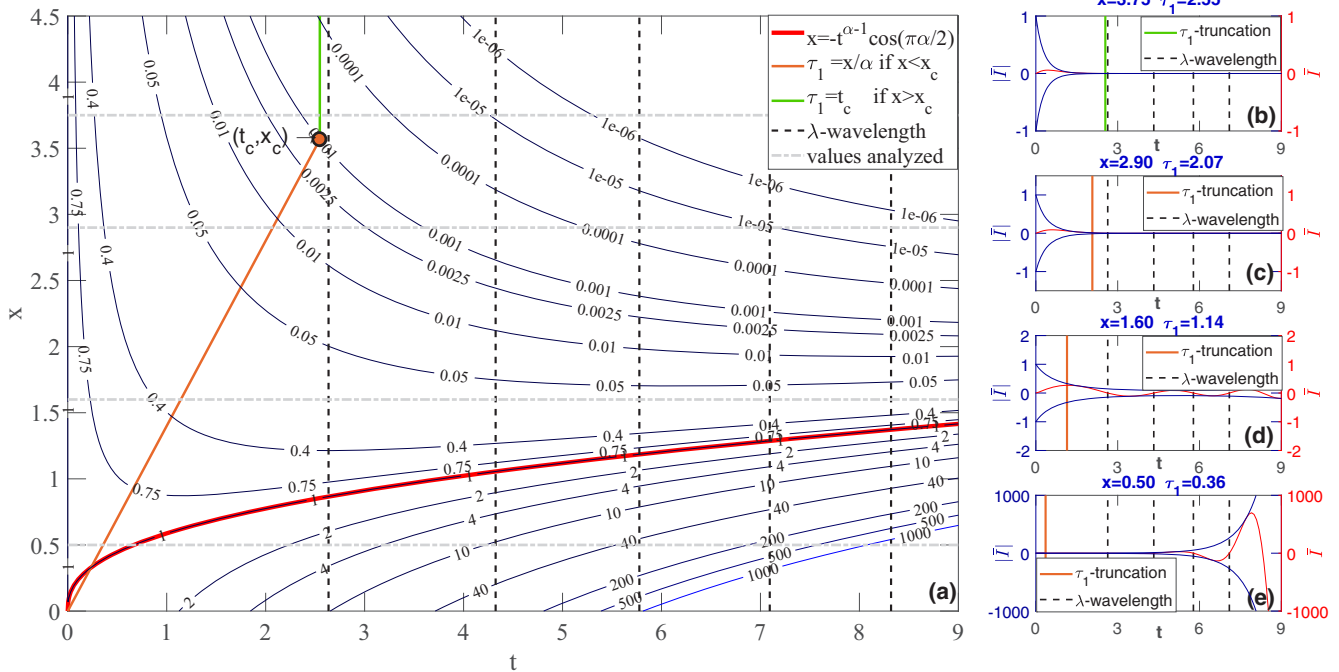


FIG. 4. Contour plot of $e^{\bar{g}}$ that represents the instantaneous amplitude $|\bar{I}|$ for $\alpha = 1.4$ and tolerance $\epsilon = 10^{-3}$ in Eqs. (31) and (32). The subfigure (a) shows the red line x which was drawn by considering $\bar{g} = 0$ representing the limit between the positive and negative values of the attenuation factor \bar{g} . The truncation τ_1 is applied following Eq. (35). Downward trend before τ_1 and upward trend after τ_1 of $|\bar{I}|$ can be observed in subfigures (d) and (e) for $x = 1.60$ and 0.50 , respectively. For $x = 2.90$ and 3.80 the truncation is made after reaching a small value on the modulation \bar{I} .

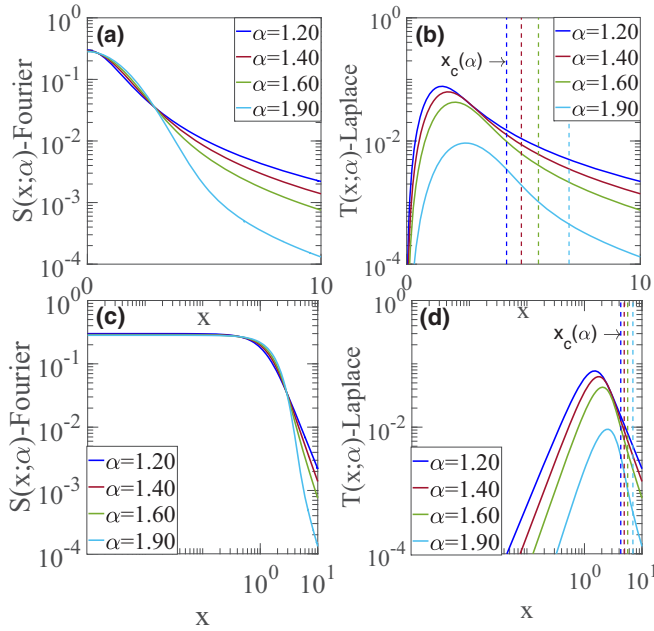


FIG. 5. Comparison of numerical integration $1 < \alpha < 2$ between the Fourier and Laplace transform of Lévy-stable $S(x; \alpha)$ and trans-stable $T(x; \alpha)$ functions using recursive adaptive Simpson quadrature method [60]. The absolute error tolerance of the method is $\xi = 3.5 \times 10^{-8}$. The subfigures (a) and (b) are shown in semilogarithmic scale and subfigures (c) and (d) are shown in logarithmic scale.

that with a small tolerance ϵ the intersection will occur in the rightmost part of the contour plot, consequently the interval of integration will be wider and a more accurate result can be obtained.

Figure 5 shows how the solutions of trans-stable and Lévy-stable distribution functions are quite similar after the x_c value, which depends on the tolerance ϵ . For a smaller ϵ the similarity of both asymptotic series is expected to improve due to a wider interval of integration. However, the value x_c will be higher and the similarity will start at the rightmost part of the axis.

V. ASYMPTOTIC EXPANSIONS

Asymptotic expansions are developed to obtain closed-form representations for the Lévy-stable distribution function $S(x, \alpha)$. These expansions are based on the Taylor series of the complex exponential function:

$$e^z \sim \sum_{k=0}^n \frac{z^k}{k!} \text{ as } n \rightarrow \infty. \tag{37}$$

Two different asymptotic expansions will be performed. The first one corresponds to the “inner expansion.” To get this solution the Lévy-stable distribution function is evaluated by expanding e^{ixt} of Eqs. (15) and (26) around $x = 0$. The second one refers to the “outer expansion,” which is the asymptotic series expansion for $x \rightarrow \infty$. When $x \gg 1$, the oscillations of the integrands in Eqs. (15) and (26) are large. Consequently, there are important cancellations due to factor e^{ixt} in the integral. Thus, we focus our integration in the region with the major contribution in the integral, that is, around $t = 0$. In

consequence, the amplitude of the integral e^{t^α} is replaced by its Taylor expansion around $t = 0$. To guarantee the convergence of the series expansion, the improper integrals are truncated. The truncation occurs because of the sufficient conditions for Riemann integral existence. These conditions are that the integrand must be bounded and the domain of integration is a closed interval [61,62].

A. Inner expansion

The inner expansion is obtained making a substitution of e^{ixt} by its Taylor series expansion given by Eq. (37) in the integrand of the Lévy-stable distribution I . After this substitution, the integrals in Eqs. (15) and (26) can be analytically solved. The difference between these two equations is the truncation on the interval of integration.

For $\alpha \leq 1$ the convergence of the series is slow, demanding a large value of order n in Eq. (37) to reach an acceptable similarity with the original integrand I . For this reason, the improper integral is truncated after a small enough amplitude of I is obtained. For $\alpha > 1$ the convergence occurs faster and truncation is not needed.

1. For $0 < \alpha \leq 1$

The inner expansion is obtained by substituting e^{ixt} in Eq. (26) by its Taylor expansion using Eq. (37). Then

$$S_i(x; \alpha, \epsilon) = \frac{1}{\pi} \int_0^{\tau_2(x, \epsilon)} e^{-t^\alpha} e^{ixt} dt \sim \frac{1}{\pi} \int_0^{\tau_2(x, \epsilon)} I_n dt \text{ as } n \rightarrow \infty, \tag{38}$$

where I_n is given by

$$I_n(x; t, \alpha) = \sum_{k=0}^n e^{-t^\alpha} \frac{(ixt)^k}{k!}. \tag{39}$$

The upper limit τ_2 is given by the following equation:

$$\tau_2(x, \epsilon) = -\frac{\ln(\epsilon)}{x}. \tag{40}$$

This truncation results from the equation $e^{ix\tau_2} = \epsilon$, where ϵ represents the tolerance that needs to be small to ensure a cutoff when negligible quantities of $|I|$ and $|I_n|$ are obtained. Consequently, the areas under the curve of both functions are similar.

The convergence of I_n to I demands a large value of order n in Eq. (37), as it can be observed in Fig. 6. This occurs because of slow decay of the e^{-t^α} value for $\alpha < 1$. This is the reason to evaluate the integral in the closed interval $[0, \tau_2]$, where the original integrand I and its Taylor series approximation I_n are similar.

The integrals in Eq. (38) can be solved without difficulty. Then, the inner expansion s_i is given by the real part of this solution:

$$s_i(x; \alpha, \epsilon) = \text{Re}[S_i(x; \alpha, \epsilon)].$$

Consequently,

$$s_i(x; \alpha, \epsilon) = \frac{1}{\pi \alpha} \sum_{k=0}^{\infty} \frac{x^k}{k!} \gamma\left(\frac{k+1}{\alpha}, \tau_2(x; \epsilon)^\alpha\right) \cos\left(\frac{\pi k}{2}\right), \tag{41}$$

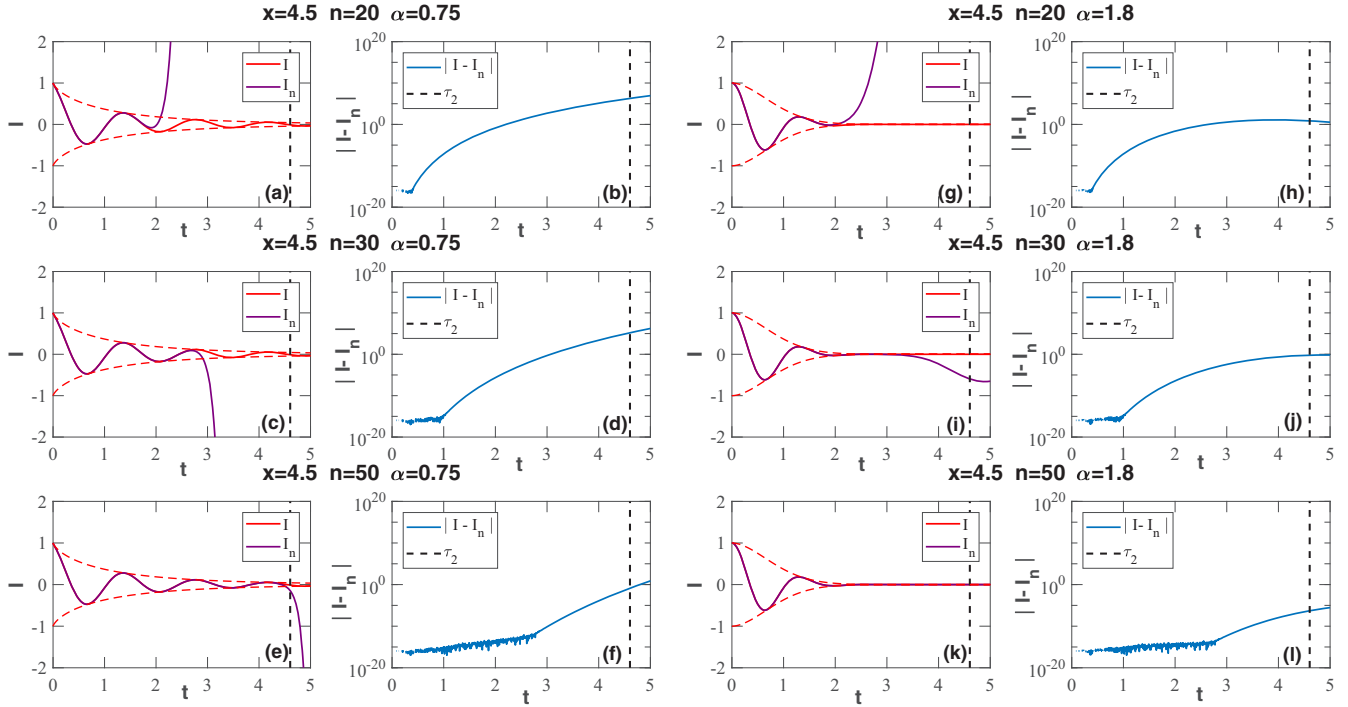


FIG. 6. Comparison of $I = e^{i^\alpha} e^{ixt}$ and $I_n = e^{i^\alpha} \sum_{k=0}^n \frac{(ixt)^k}{k!}$ of Eqs. (38) and (43), where I_n is obtained by replacing e^{ixt} in I by its Taylor expansion. The plots are for $\alpha = 0.75$ in the subfigures (a)–(f) and $\alpha = 1.8$ in the subfigures (g)–(l). For $\alpha \leq 1$, the truncation is required to ensure a cutoff when negligible quantities of $|I|$ and $|I_n|$ are obtained. The truncated error of the Taylor expansion is measured by using the absolute value of the difference $|I - I_n|$. For $\alpha > 1$, since the convergence is fast the truncation is unnecessary. For these particular examples, the integrand I is evaluated at $x = 4.5$ for three cases of $n = 20, 30$, and 50 with $\epsilon = 10^{-9}$.

where γ represents the incomplete gamma function [63]:

$$\gamma(z, b) = \int_0^b x^{z-1} e^{-x} dx. \quad (42)$$

Due to a computation of the incomplete gamma function γ , Eq. (41) was modified for numerical analysis in MATLAB²

2. For $1 < \alpha < 2$

Here we derive the inner expansion s_i for $\alpha > 1$ from the nontruncated form of the Lévy-stable distribution function. This derivation is made by substituting e^{ixt} in Eq. (15) by its Taylor expansion in Eq. (37), then

$$S_i(x; \alpha) = \frac{1}{\pi} \int_0^\infty e^{-t^\alpha} e^{ixt} dt \sim \frac{1}{\pi} \int_0^\infty I_n dt \quad \text{as } n \rightarrow \infty. \quad (43)$$

For $\alpha > 1$, the convergence of integrand I and the integrand after the substitution I_n occurs faster than for $\alpha < 1$. This feature is observed in Fig. 6, where an acceptable convergence

between I and I_n is obtained with a small n value. Consequently, the integral is evaluated without truncation or taking the limit $\epsilon \rightarrow 0$ in Eq. (38).

Then, we only consider the real part of the solution of Eq. (43):

$$s_i(x; \alpha) = \text{Re}[S_i(x; \alpha)].$$

Consequently,

$$s_i(x; \alpha) = \frac{1}{\pi \alpha} \sum_{k=0}^\infty \frac{x^k}{k!} \Gamma\left(\frac{k+1}{\alpha}\right) \cos\left(\frac{\pi k}{2}\right), \quad (44)$$

where Γ represents the gamma function [63]:

$$\Gamma(b) = \int_0^\infty x^{b-1} e^{-x} dx.$$

Examples for $\alpha = 0.75$ and 1.80 are shown in Figs. 7 and 8, respectively. In Fig. 7, for $\alpha \leq 1$ the truncation τ_2 is needed, otherwise the convergence to the Lévy-stable distribution function will be ultraslow as $n \rightarrow \infty$. This is evident when a comparison is made between Figs. 7(a) and 7(b). They represent a nontruncated and truncated Lévy-stable solution, respectively. Figure 7(b) displays an acceptable convergence with a smaller order n . In Fig. 8, for $\alpha > 1$ the convergence to the Lévy-stable distribution function occurs faster and no truncation is needed. For both cases the inner expansion s_i behaves well because it converges to $s(x; \alpha)$.

²MATLAB defines the incomplete gamma function as γ^* :

$$\gamma^*(b, z) = \frac{1}{\Gamma(z)} \int_0^z x^{z-1} e^{-x} dx,$$

where $\Gamma(z)$ is the gamma function. [64].

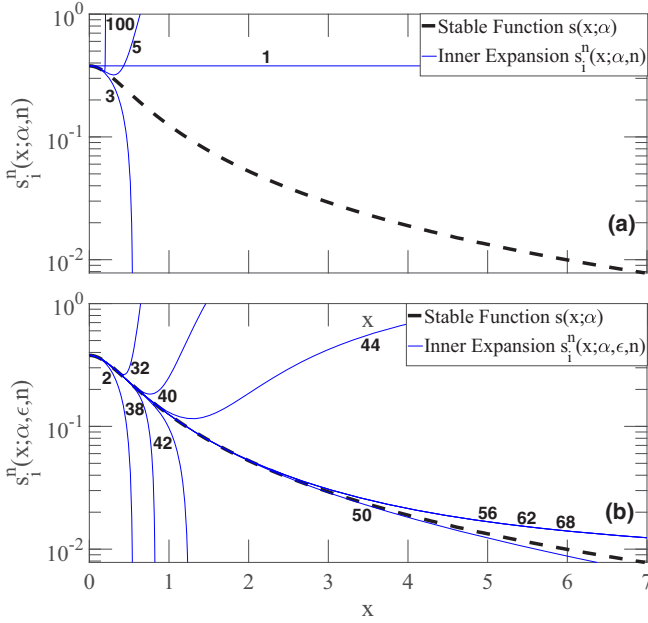


FIG. 7. Inner expansion of the Lévy-stable distribution function for $\alpha = 0.75$. This is obtained by applying Taylor expansion around $t = 0$. The subfigure (a) is a nontruncated integral. The subfigure (b) is the truncated integral with tolerance $\epsilon = 10^{-9}$ in Eq. (41), which displays a fast convergence due to the integral’s truncation.

B. Outer expansion

The outer expansion is obtained making a substitution of the amplitude e^{-t^α} in the integrand of the truncated Lévy-stable distribution function I in Eq. (26) by its Taylor series expansion around $t = 0$. Then, the following relation is obtained:

$$S_o(x; \alpha, \epsilon) = \frac{1}{\pi} \int_0^{\tau_3(\epsilon)} e^{-t^\alpha} e^{ixt} dt \sim \frac{1}{\pi} \int_0^{\tau_3(\epsilon)} G_n dt \text{ as } n \rightarrow \infty, \quad (45)$$

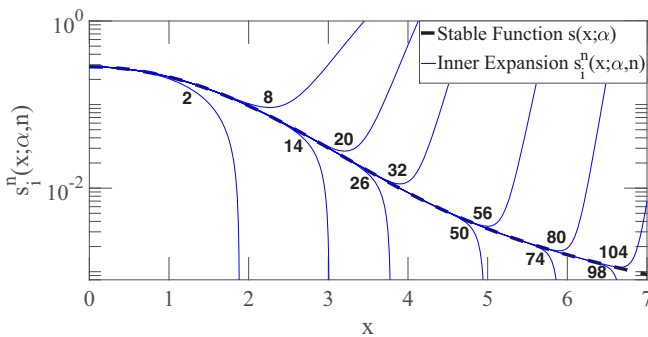


FIG. 8. Inner expansion of the Lévy-stable distribution for $\alpha = 1.80$ as a result of applying a Taylor expansion in the “exponential of the phase” of the integrand. The figure illustrates the nontruncated Lévy-stable solution in Eq. (44). This figure displays a fast convergence so that no truncation is needed.

where G_n is given by

$$G_n(x; \alpha) = \sum_{k=0}^n \frac{(-t^\alpha)^k}{k!} e^{ixt}. \quad (46)$$

The upper limit τ_3 is given by the following equation:

$$\tau_3(\epsilon) = [-\ln(\epsilon)]^{1/\alpha}. \quad (47)$$

This truncation is calculated from $e^{-\tau_3^\alpha} = \epsilon$, where ϵ is defined as tolerance and represents a negligible instantaneous amplitude when ϵ is small. The truncation allows a faster convergence of G_n to I and reduces the error of integration due to an accurate approximation on the interval $[0, \tau_3]$.

The original integrand I and the new integrand after applying Taylor series G_n in Eq. (45) were evaluated in Fig. 9. Since the convergence of G_n to I is slow, the truncation τ_3 is considered to define the new interval of integration $[0, \tau_3]$.

To obtain the outer solution s_o a change of variable after the series expansion is applied in Eq. (45). The change of variable is $-u = ixt$, so $-du = ixdt$. This gives us an approximation of the form

$$S_o(x; \alpha, \epsilon) \sim \frac{1}{\pi} \sum_{k=0}^n \frac{(-1)^k}{k!} \left(\frac{-1}{ix}\right)^{k\alpha+1} \int_0^{-ix\tau_3(\epsilon)} u^{k\alpha} e^{-u} du. \quad (48)$$

To solve the integral, the incomplete gamma function of imaginary argument $\gamma(v, iz)$ is used [63,65]. The following solution is presented by Barakat as a special case of the confluent hypergeometric function [65]:

$$\begin{aligned} \gamma(v, iz) &= \int_0^{iz} t^{v-1} e^{-t} dt \\ &= (iz)^v v^{-1} {}_1F_1(v, 1+v, -iz), \end{aligned} \quad (49)$$

where ${}_1F_1(v, 1+v, -iz)$ represents the confluent hypergeometric function. Then, comparing Eqs. (48) and (49), we obtain the following relation between the variables, $v = k\alpha + 1$, $z = -x\tau_3$, and $t = u$.

Finally, the real part of the solution is

$$s_o(x; \alpha, \epsilon) = \text{Re}[S_o(x; \alpha, \epsilon)].$$

Consequently,

$$\begin{aligned} s_o(x; \alpha, \epsilon) &= -\frac{1}{\pi} \sum_{k=1}^{\infty} \frac{(-1)^k}{k!} \left(\frac{\cos(\pi\alpha k)}{k\alpha + 1}\right) \dots \\ &\times [-\tau_3(\epsilon)]^{k\alpha+1} {}_1F_1(k\alpha + 1, k\alpha + 2, ix\tau_3(\epsilon)). \end{aligned} \quad (50)$$

Figure 10 shows the calculation of Eq. (50) for $\alpha = 1.8$. In this figure is evident that the outer expansion s_o converges slowly. This occurs due to computation of the confluent hypergeometric function ${}_1F_1$ which demands considerable computational time. The series that defines the function ${}_1F_1$ does not have a trivial structure, which creates numerical issues which makes the calculation computationally inefficient [66]. The approximation in Fig. 10 shows how the convergence demands a large value of order n to obtain an accurate approximation at the tail. The convergence resembles waves that slowly start to decrease from the tails to the peak of the Lévy-stable distribution. The

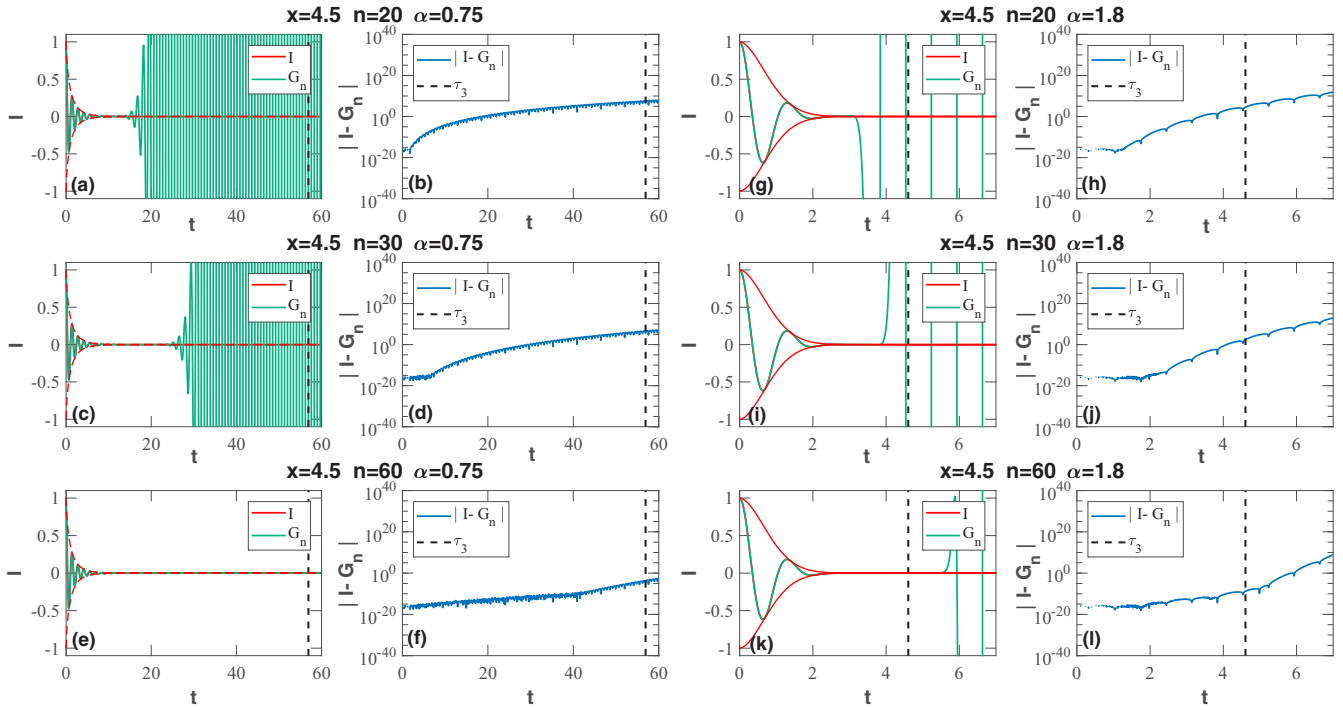


FIG. 9. Comparison of $I = e^{t^\alpha} e^{ixt}$ and $G_n = \sum_{k=0}^n \frac{(-it)^{\alpha k}}{k!} e^{ixt}$ of Eq. (45), where G_n is the Taylor expansion of I around $t = 0$. The plots are for $\alpha = 0.75$ in the subfigures (a)–(f) and $\alpha = 1.8$ in the subfigures (g)–(l). Truncation of the integral is required for both cases. The reason of that is to reach an accurate approximation between the original integrand I and the one after the series expansion G_n . The error is measured by the absolute value of the difference $|I - G_n|$. For these particular examples, the integrand I is evaluated at $x = 4.5$ for three cases of $n = 20, 30$, and 50 with $\epsilon = 10^{-9}$.

series until $n = 30$ does not show an acceptable approximation. Only an approximation on tails is obtained after $n = 40$. For $x \rightarrow 0$, the series of s_o converges to a specific value different from the Lévy-stable distribution function. The convergence

to the Lévy-stable distribution function is observed only for $x \rightarrow \infty$.

C. Outer expansion by trans-stable distribution

Because of the slow convergence of the outer expansion s_o and its wavelike behavior, an alternative approximation is obtained using the trans-stable function $T(x; \alpha)$. As it was previously explained in Sec. IV, the solutions of trans-stable $T(x; \alpha)$ and Lévy-stable $S(x; \alpha)$ functions are identical for $0 < \alpha \leq 1$ and similar for $1 < \alpha < 2$ after the x_c value. Consequently, the improper integral in Eq. (24) is used to calculate the series expansions for $0 < \alpha \leq 1$ and the truncated trans-stable integral in its Laplace representation in Eq. (29) for $1 < \alpha < 2$.

This outer expansion t_o is given by the analytical solution of the trans-stable function after applying the Taylor series of $e^{-(it)^\alpha}$ around $t = 0$ in the trans-stable integrand \bar{I} using Eqs. (37) and (24). Then, the following equation is shown:

$$T_o(x; \alpha, \epsilon) = \frac{1}{\pi} \int_0^{\tau_1(x, \epsilon)} e^{-(it)^\alpha} e^{-xt} i dt \sim \frac{1}{\pi} \int_0^{\tau_1(x, \epsilon)} K_n dt, \quad (51)$$

where K_n is given by

$$K_n(x) = \sum_{k=0}^n \frac{(-it)^{\alpha k}}{k!} e^{-xt} i. \quad (52)$$

Due to a slow convergence of K_n to \bar{I} the cutoff τ_1 is applied. The truncation τ_1 has two different expressions. For $\alpha \leq 1$,

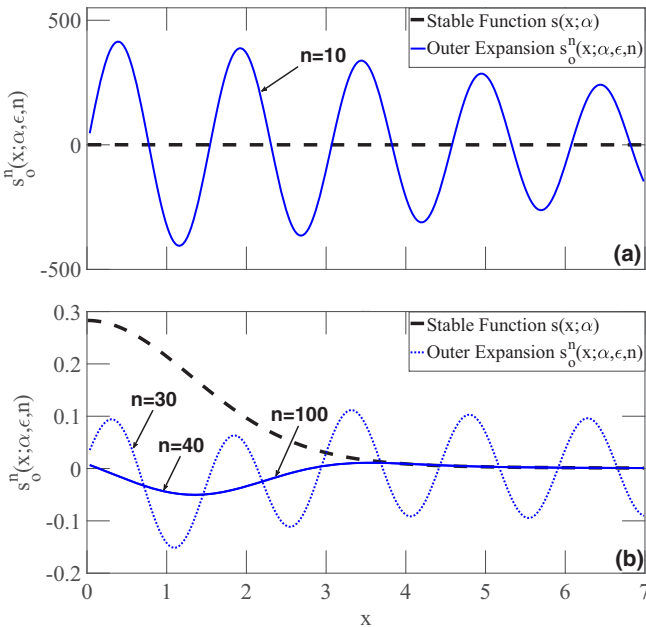


FIG. 10. Outer expansion s_o for $\alpha = 1.80$ with tolerance $\epsilon = 10^{-6}$ in Eq. (50). The subfigures (a) and (b) correspond to $n = 10, 30, 40$, and 100 , respectively.

the truncation τ_1 depends on the tolerance ϵ and for $\alpha > 1$ it depends on the tolerance ϵ and x values. These expressions will be explained in the following subsections.

To solve the integral in Eq. (51), the following change of variable is applied: $xt = u$ and $xdt = du$. This leads to the following series expansion:

$$T_o(x; \alpha, \epsilon) \sim \frac{1}{\pi} \sum_{k=0}^{\infty} \frac{(-1)^k}{k!} \left(\frac{-1}{ix}\right)^{k\alpha+1} \times \int_0^{x\tau_1(x, \epsilon)} u^{(k\alpha+1)-1} e^{-u} du. \quad (53)$$

The upper limit of the integral changes from τ_1 to $x\tau_1$, but still remains on the real axis. The integral above can be solved using the incomplete gamma function defined in Eq. (42). Then, the real part of the result is obtained:

$$t_o(x; \alpha, \epsilon) = \text{Re}[T_o(x; \alpha, \epsilon)].$$

Consequently,

$$t_o(x; \alpha, \epsilon) = -\frac{1}{\pi} \sum_{k=1}^{\infty} \frac{(-1)^k}{k!} \left(\frac{1}{x}\right)^{k\alpha+1} \times \sin\left(\frac{\pi\alpha k}{2}\right) \gamma(k\alpha + 1, x\tau_1(x, \epsilon)). \quad (54)$$

The determination of τ_1 for $\alpha \leq 1$ and $\alpha > 1$ is presented in the following subsections.

1. For $0 < \alpha \leq 1$

For $\alpha \leq 1$, the cutoff τ_1 in Eq. (54) is given by the following equation:

$$\tau_1(\epsilon) = [-\ln(\epsilon)]^{1/\alpha} \text{ for } \alpha \leq 1. \quad (55)$$

This truncation is obtained from $e^{-\tau_1^\alpha} = \epsilon$, where the tolerance ϵ represents a negligible instantaneous amplitude for the integrands in Eq. (51).

2. For $1 < \alpha < 2$

The truncation τ_1 in Eq. (54) for $1 < \alpha < 2$ was already obtained in Sec. IV B and defined by Eq. (35) as

$$\tau_1(x, \epsilon) = \begin{cases} t_c(\epsilon) & \text{if } x > x_c, \\ x/\alpha & \text{if } x < x_c, \end{cases} \text{ for } \alpha > 1,$$

where t_c and x_c were defined by Eq. (36). As indicated in Sec. IV B, the value of τ_1 is used to minimize the truncation error and at the same time to make the domain of integration as small as possible.

The outer expansion by the trans-stable function converges to the original trans-stable function. Examples are shown in Fig. 11 for $\alpha \leq 1$ and Fig. 12 for $\alpha > 1$. Note that in both cases the truncation τ_1 allows a faster and more accurate convergence to the real part of the trans-stable distribution $t(x; \alpha)$. Consequently the outer solution t_o shows an identical solution as $s(x; \alpha)$ for $\alpha \leq 1$ and the same asymptotic behavior for $\alpha > 1$. For a smaller ϵ the convergence of these outer expansions to the trans-stable function will occur faster. Also

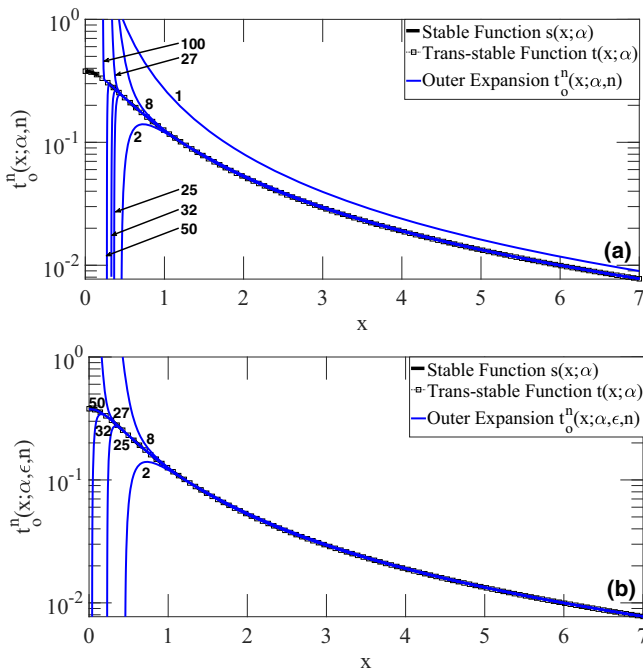


FIG. 11. Outer expansion of the trans-stable function for $\alpha = 0.75$. This result is obtained from the Taylor expansion of the integrand around $t = 0$ in Eqs. (54) and (55). The subfigure (a) is the nontruncated integral that shows slow convergence. The subfigure (b) corresponds to the truncated integral with tolerance $\epsilon = 10^{-6}$. The subfigure (b) displays a faster convergence to the trans-stable function as a result of the truncation of the integral.

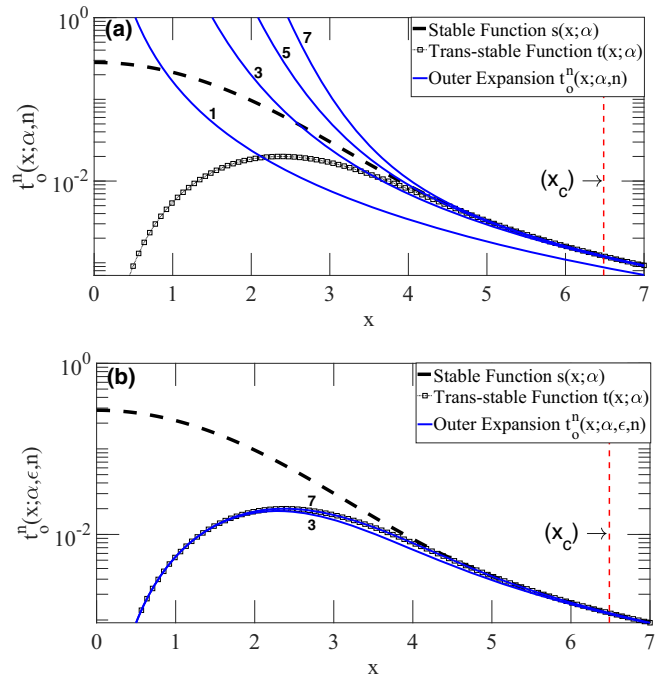


FIG. 12. Outer expansion of the trans-stable function for $\alpha = 1.80$ as a result of applying Taylor expansion of the integrand around $t = 0$ in Eqs. (35) and (54). The subfigure (a) shows that the nontruncated integral does not converge to the trans-stable function. The subfigure (b) corresponds to the truncated integral with tolerance $\epsilon = 10^{-6}$. The subfigure (b) displays a fast convergence as a result of the truncation of the integral.

TABLE II. Summary of inner and outer expansions.

Range of α	$0 < \alpha \leq 1$	$1 < \alpha < 2$
Normalized Lévy-stable distribution (s)	$s(x; \alpha) = \frac{1}{\pi} \int_0^\infty e^{-t^\alpha} \cos(tx) dt$	
Normalized trans-stable distribution (t)	$t(x; \alpha) = \frac{1}{\pi} \int_0^\infty e^{-t^\alpha \cos(\frac{\pi x}{2}) - xt} \sin[t^\alpha \sin(\frac{\pi x}{2})] dt$	
Inner expansion (s_i^n)	$s_i^n(x; \alpha, \epsilon) = \frac{1}{\pi \alpha} \sum_{k=0}^n \frac{x^k}{k!} \gamma(\frac{k+1}{\alpha}, \tau_2^\alpha) \cos(\frac{\pi k}{2})$	$s_i^n(x; \alpha) = \frac{1}{\pi \alpha} \sum_{k=0}^n \frac{x^k}{k!} \Gamma(\frac{k+1}{\alpha}) \cos(\frac{\pi k}{2})$
	$\tau_2 = \frac{-\ln(\epsilon)}{x}$	
Outer expansion (s_o^n)	$s_o^n(x; \alpha, \epsilon) = -\frac{1}{\pi} \sum_{k=1}^n \frac{(-1)^k}{k!} \left(\frac{\cos(\pi \alpha k)}{k \alpha + 1}\right) (-\tau_3)^{k \alpha + 1} {}_1F_1(k \alpha + 1, k \alpha + 2, i x \tau_3)$	
	$\tau_3 = [-\ln(\epsilon)]^{1/\alpha}$	
Outer expansion ^a (t_o^n)	$t_o^n(x; \alpha, \epsilon) = -\frac{1}{\pi} \sum_{k=1}^n \frac{(-1)^k}{k!} \left(\frac{1}{x}\right)^{k \alpha + 1} \gamma(k \alpha + 1, x \tau_1) \sin(\frac{\pi \alpha k}{2})$	
	$\tau_1 = [-\ln(\epsilon)]^{1/\alpha}$	$\tau_1 = \begin{cases} t_c & \text{if } x > x_c \\ x/\alpha & \text{if } x < x_c \end{cases}$
Complete and incomplete gamma functions (Γ and γ)	$\Gamma(z) = \int_0^\infty x^{z-1} e^{-x} dx \quad \gamma(z, b) = \int_0^b x^{z-1} e^{-x} dx$	

^aRefer to Eq. (35) to obtain the t_c and x_c value for $1 < \alpha < 2$.

in Fig. 11 the nontruncated trans-stable expansion is shown as an expansion that converges extremely slowly requiring a higher order n than truncated trans-stable expansion to obtain an acceptable convergence. In Fig. 12 the nontruncated trans-stable expansion does not converge to the trans-stable function at all.

VI. UNIFORM SOLUTION

The uniform solution is presented as the combination of the inner solution and the outer solution to construct an approximation valid for all $x \in [-\infty, \infty]$. To construct the uniform solution an asymptotic matching method based on boundary-layer theory is applied [67,68]. This method is based on superposing the inner and outer solution and subtracting the overlap between them:

$$s_u(x) = y_{out}(x) + y_{in}(x) - y_{overlap}(x). \tag{56}$$

The overlap is defined as the limit of the rightmost edge of y_{in} and the leftmost edge of y_{out} :

$$y_{overlap} = \lim_{x \rightarrow 0} y_{out} = \lim_{x \rightarrow \infty} y_{in}. \tag{57}$$

For this case, our proposed uniform solution s_u is constructed based on our inner expansion s_i and our outer expansion t_o . These previous solutions were already defined in Sec. V.

For a better understanding of our uniform solution s_u , two subsections are presented. Section VIA contains a summary of inner and outer expansions previously obtained. In Sec. VIB the steps taken to obtain s_u are explained.

A. Summary of inner and outer expansions

Table II contains the normalized Lévy-stable and trans-stable distribution and the summary of previous results obtained from Lévy-stable and trans-stable functions by applying Taylor expansions. The series refers to one inner expansion s_i and two outer expansions s_o and t_o .

For the inner expansion s_i , the solution for $\alpha \leq 1$ corresponds to a truncated Lévy-stable solution which allows a faster convergence. For $\alpha > 1$ the series is obtained from the nontruncated Lévy-stable solution. The only difference between them is the use of the incomplete gamma function γ in the solution for $\alpha \leq 1$, where $\Gamma(z) = \lim_{b \rightarrow \infty} \gamma(z, b)$. Consequently, for both cases the truncated series can provide a good approximation. However, in the case of $\alpha \leq 1$ we must take the limit as

$$s(x; \alpha) = \lim_{\epsilon \rightarrow 0} \left[\lim_{n \rightarrow \infty} s_i^n(x; \alpha, \epsilon) \right] \text{ for } x < \infty.$$

In general the order in which we apply the limits cannot be exchanged. However, in the case of $\alpha > 1$ the order of the limits does not affect the convergence. Taking a small value of ϵ ensures a faster convergence.

For the outer expansion two expressions were derived. The first outer expansion s_o is obtained by performing the Taylor expansion around $t = 0$ on the truncated Lévy-stable distribution. This solution displays a slow convergence for $n \rightarrow \infty$. The second outer expansion t_o is obtained by applying the Taylor expansion on the truncated trans-stable function for $x \rightarrow \infty$. The truncation of t_o depends on α and there are two different cases. For $\alpha \leq 1$ it converges to the exact solution of $s(x; \alpha)$ and for $\alpha > 1$ it converges to the same solution at the tails of $s(x; \alpha)$. To guarantee convergence, we need to take the limit as

$$t(x; \alpha) = \lim_{\epsilon \rightarrow 0} \left[\lim_{n \rightarrow \infty} t_o^n(x; \alpha, \epsilon) \right] \text{ for } x > 0.$$

Exchanging the order of the limits will affect the convergence. The outer expansion that will be used is t_o , because it displays a faster convergence and it does not exhibit wavelike behavior.

B. Steps to obtain the uniform solution

To obtain the uniform solution s_u the condition in Eq. (57) needs to be satisfied. The inner expansion s_i and the outer

expansion t_o have to be multiplied with an appropriate coefficient $A(x)$ to obtain the asymptotic solutions with a common matching value y_m . These operations will allow us to obtain y_{out} and y_{in} . Consequently, Eq. (56) will be applied to obtain the closed-form solution of the Lévy-stable distribution function.

Below, the steps are explained to obtain the location of the matching between the inner and the outer solutions (x_m, y_m) , the coefficient $A(x)$, and the uniform solution s_u .

1. Finding the inner and outer limit (x_m, y_m)

Considering s_i and t_o as good approximations to the Lévy-stable distribution function, we must require that the inner and the outer expansions will be close enough before matching them [69]. Consequently, the point where the matching between s_i and t_o takes place is (x_m, y_m) and it represents the location where the minimal vertical distance between the inner s_i and the outer solution t_o occurs.

The distance function between s_i and s is defined as δ_i and the distance function between t_o and s is δ_o . Consequently, (x_m, y_m) is the point where the Pythagorean addition of these distances is minimal:

$$\begin{aligned} \delta_i^2(x; \alpha, \epsilon) &= [s(x; \alpha) - s_i(x; \alpha, \epsilon)]^2, \\ \delta_o^2(x; \alpha, \epsilon) &= [s(x; \alpha) - t_o(x; \alpha, \epsilon)]^2, \\ \delta^2(x; \alpha, \epsilon) &= \delta_o^2(x; \alpha, \epsilon) + \delta_i^2(x; \alpha, \epsilon), \end{aligned}$$

$$\left. \frac{d[\delta^2(x; \alpha, \epsilon)]}{dx} \right|_{x_m} = 0. \tag{58}$$

The x_m value is obtained from the previous equation. Then, y_m is defined by the equidistant point between both functions:

$$y_m = \frac{s_i(x_m) + t_o(x_m)}{2}. \tag{59}$$

2. Defining the inner and outer solutions y_{in} and y_{out}

To obtain the uniform solution s_u , the asymptotic matching method based on the boundary-layer theorem [67] is applied. Consequently, the inner solution y_{in} and the outer solution y_{out} must have a matching asymptotic behavior. More precisely, the limit of the outer solution y_{out} when $x \rightarrow 0$ should correspond to the limit of the inner solution y_{in} when $x \rightarrow \infty$. To obtain y_{in} and y_{out} solutions, the series expansions s_i and t_o are multiplied by appropriate coefficients to meet the requirements of matching asymptotic expansions, so the y_{in} and y_{out} are defined as follows:

$$y_{in}(x; \alpha, \epsilon, \mu) = [s_i(x) - y_m][1 - A(x; \mu)] + y_m, \tag{60}$$

$$y_{out}(x; \alpha, \epsilon, \mu) = [t_o(x) - y_m]A(x; \mu) + y_m, \tag{61}$$

where the overlapping factor $A(x)$ is defined as

$$A(x; \mu) = \frac{1}{2} \left[1 + \tanh \left(\frac{x - x_m}{\mu} \right) \right]. \tag{62}$$

The $A(x; \mu)$ is used to smooth s_i and t_o and provides them with a symmetric overlap section around x_m and gives y_{in} and y_{out} an asymptotic behavior. The variable μ determines the width of the overlap between y_{in} and y_{out} .

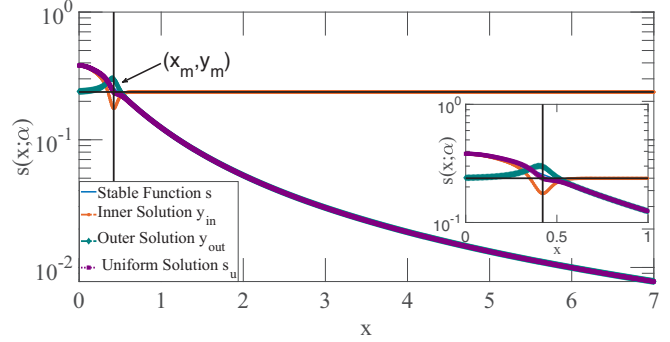


FIG. 13. Uniform solution s_u for $\alpha = 0.75$ as a result of joining the inner solution y_{in} with the outer solution y_{out} . The tolerance $\epsilon = 10^{-6}$, $\mu = 0.052$, and $n_i = 6$ and $n_o = 17$.

It is easy to see that Eqs. (60) and (61) satisfy Eq. (57), where the limits of y_{out} and y_{in} converge to a constant value y_m .

3. Defining the uniform solution s_u

The inner solution y_{in} Eq. (60) and the outer solution y_{out} in Eq. (61) were defined to fulfill the requirements for matching asymptotic expansions. Then, Eq. (56) is applied to obtain the uniform solution s_u :

$$\begin{aligned} s_u^{n_i, n_o}(x; \alpha, \epsilon, \mu) &= \frac{t_o^{n_o}(x; \alpha, \epsilon)}{2} + \frac{s_i^{n_i}(x; \alpha, \epsilon)}{2} + \tanh \left(\frac{x - x_m}{\mu} \right) \\ &\quad \times \left(\frac{t_o^{n_o}(x; \alpha, \epsilon)}{2} - \frac{s_i^{n_i}(x; \alpha, \epsilon)}{2} \right). \end{aligned} \tag{63}$$

4. Find the best s_u by choosing the most appropriate μ

The width of the overlap between y_{in} and y_{out} can be optimized to obtain the closest solution s_u of the Lévy-stable distribution function. The most appropriate value of μ needs to be obtained for each particular value of α . For that, the least square method will be applied between the original $s(x; \alpha)$ and the new closest solution $s_u(x; \alpha, \epsilon, \mu)$. Applying Eqs. (12) and (63) the following equation is obtained:

$$L(\mu) = \sum_{i=1}^N [s_u(x_i; \alpha, \epsilon, \mu) - s(x_i; \alpha)]^2, \tag{64}$$

where the N value represents the length of the sample used to minimize L .

The similarity between the exact solution of $s(x; \alpha)$ and the uniform solution $s_u(x; \alpha, \epsilon, \mu)$ is observed in Figs. 13 and 14 for $\alpha = 0.75$ and 1.80, respectively. For $\alpha < 1$, a good approximation between $s(x; \alpha)$ and $s_u(x; \alpha, \epsilon, \mu)$ is obtained in the tails after mixing two different orders. The order for the inner solution is $n_i = 6$, which makes the solution concave upward. The order for the outer solution is $n_o = 17$, which makes the solution concave downward. This combination of orders will ensure a good matching asymptotic behavior. For $\alpha > 1$, the uniform solution works well, and a good uniform solution is obtained quickly with a lower order $n = 6$.

Lower orders can be used for both cases, where the most important aspect to consider is the different concavity between y_{in}

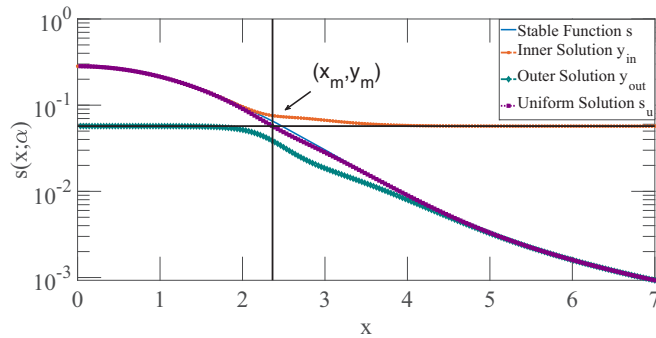


FIG. 14. Uniform solution s_u for $\alpha = 1.80$ as a result of joining the inner solution y_{in} with the outer solution y_{out} . The tolerance $\epsilon = 10^{-6}$, $\mu = 0.4$, and $n = 8$.

and y_{out} for the matching asymptotic behavior. The concavity of the inner and outer solution is defined by the trigonometric element in each solution.

VII. CONCLUSIONS

In this paper we presented a uniform solution of the Lévy-stable distribution. This solution converges to the Lévy-stable distribution function in the full range of x values $-\infty < x < \infty$. This condition makes our uniform solution more robust than previous analytical expressions that were only applicable for extreme values $x \rightarrow 0$ or ∞ . Also, our uniform solution removes the negative values obtained in previous numerical solutions of the Lévy-stable distribution function for all α values, which makes this solution more reliable because a probability density function must be always positive.

The uniform solution is the result of an asymptotic matching between the inner and outer expansions. The inner expansion results from the Taylor series expansion of the characteristic function of the Lévy-stable distribution around $x = 0$. The outer expansion is obtained from the Taylor expansion of the integrand of the trans-stable function around $t = 0$. The convergence of these expansions is guaranteed if the integrands are truncated, and the speed of convergence depends on how the truncation is implemented.

For $\alpha \leq 1$, the uniform solution provides a good approximation for the full range of x values. Also, the numerical integration of the trans-stable function constitutes a second option which allows us to obtain a robust numerical solution of the Lévy-stable distribution function and removes the oscillations. For $\alpha > 1$, the uniform solution provides an analytical solution of the Lévy-stable distribution function based on fast converging series. Consequently, the closed-form solution presented in this paper will provide an analytical solution of the fractional kinetic equations (FDE, FDAE, and FFPE).

Additionally, having an analytical solution for the Lévy-stable distribution will contribute to modeling stock markets. To achieve this, Lévy-stable noise will be generated numerically. The following procedure is described to generate Lévy-stable noise. First random points between zero and one are generated. Then, the inverse of the cumulative distribution function of the Lévy-stable distribution is applied to these points. Consequently, the corresponding image of the uniformly generated points will be Lévy-stable distributed. Different compromises between accuracy and efficiency in the random number generation can be attained by changing the order n in Eq. (63). Hence, a computational efficiency and high precision are achieved during the generation of large sets of points.

For modeling stock markets, Lévy-stable noise represents the net trading volume—the difference between buy and sell stocks’ volume—and will feed macroscopic models of the stock markets. On the other hand, to develop a microscopic model of stock markets, the Lévy-stable noise can be used to represent the order book (OB)—the list of request for buy and sell orders with prices and volumes. The use of Lévy-stable noise is justified by the fact that volumes, lifetime of orders, and the placement of limit orders in a OB present power-law decays with a characteristic exponent—stability parameter α —which belongs to Lévy-stable distribution function.

ACKNOWLEDGMENTS

F.A.-M. thanks Hans J. Herrmann for useful discussions and his hospitality in ETH Zürich, Switzerland. K.A.-C. thanks The Sydney Informatics Hub at The University of Sydney for providing access to the high-performance computer (HPC-Artemis) to test our uniform solution.

[1] D. L. Turcotte, Self-organized criticality, *Rep. Prog. Phys.* **62**, 1377 (1999).
 [2] B. D. Malamud, Tails of natural hazards, *Phys. World* **17**, 25 (2004).
 [3] G. Samorodnitsky and M. S. Taqqu, *Stable Non-Gaussian Random Processes: Stochastic Models with Infinite Variance* (Chapman & Hall—One Penn Plaza, New York, 1994).
 [4] P. Gopikrishnan, V. Plerou, Yan Liu, L. A. N. Amaral, X. Gabaix, and H. E. Stanley, Scaling and correlation in financial time series, *Physica A* **287**, 362 (2000).
 [5] O. Biham, Zhi-Feng Huang, O. Malcai, and S. Solomon, Long-time fluctuations in a dynamical model of stock market indices, *Phys. Rev. E* **64**, 026101 (2001).
 [6] A. Nobl, S. E. Maeng, G. G. Ha, and J. W. Lee, Effects of global financial crisis on network structure in a local stock market, *Physica A* **407**, 135 (2014).
 [7] S. Borak, W. Hardle, and R. Weron, Stable distributions, in *Statistical Tools for Finance and Insurance* (Springer, New York, 2005), pp. 21–44.
 [8] Y. Yuan, Xin-tian Zhuang, X. Jin, and Wei-qiang Huang, Stable distribution and long-range correlation of Brent crude oil market, *Physica A* **413**, 173 (2014).
 [9] S. C. Lera and D. Sornette, Gross domestic product growth rates as confined Lévy flights: Towards a unifying theory of economic growth rate fluctuations, *Phys. Rev. E* **97**, 012150 (2018).
 [10] V. Plerou and H. E. Stanley, Tests of scaling and universality of the distributions of trade size and share volume: Evidence from three distinct markets, *Phys. Rev. E* **76**, 046109 (2007).
 [11] V. Plerou and H. E. Stanley, Reply to “Comment on ‘Tests of scaling and universality of the distributions of trade size and share volume: Evidence from three distinct markets’”, *Phys. Rev. E* **79**, 068102 (2009).

- [12] M. Magdziarz, S. Orzeł, and A. Weron, Option pricing in subdiffusive Bachelier model, *J. Stat. Phys.* **145**, 187 (2011).
- [13] Y. Yura, H. Takayasu, D. Sornette, and M. Takayasu, Financial Brownian Particle in the Layered Order-Book Fluid and Fluctuation-Dissipation Relations, *Phys. Rev. Lett.* **112**, 098703 (2014).
- [14] R. Friedrich, J. Peinke, and Ch. Renner, How to Quantify Deterministic and Random Influences on the Statistics of the Foreign Exchange Market, *Phys. Rev. Lett.* **84**, 5224 (2000).
- [15] R. Metzler, E. Barkai, and J. Klafter, Anomalous Diffusion and Relaxation Close to Thermal Equilibrium: A Fractional Fokker-Planck Equation Approach, *Phys. Rev. Lett.* **82**, 3563 (1999).
- [16] R. Metzler and J. Klafter, The random walk's guide to anomalous diffusion: A fractional dynamics approach, *Phys. Rep.* **339**, 1 (2000).
- [17] R. Metzler and J. Klafter, The restaurant at the end of the random walk: Recent developments in the description of anomalous transport by fractional dynamics, *J. Phys. A* **37**, R161 (2004).
- [18] R. Jain and K. L. Sebastian, Lévy flight with absorption: A model for diffusing diffusivity with long tails, *Phys. Rev. E* **95**, 032135 (2017).
- [19] A. S. Chaves, A fractional diffusion equation to describe Lévy flights, *Phys. Lett. A* **239**, 13 (1998).
- [20] C. Tsallis, S. V. F. Levy, A. M. C. Souza, and R. Maynard, Statistical-Mechanical Foundation of the Ubiquity of Lévy Distributions in Nature, *Phys. Rev. Lett.* **75**, 3589 (1995).
- [21] D. Janakiraman and K. L. Sebastian, Path-integral formulation for Lévy flights: Evaluation of the propagator for free, linear, and harmonic potentials in the over- and underdamped limits, *Phys. Rev. E* **86**, 061105 (2012).
- [22] A. Kamińska and T. Srokowski, Lévy walks in nonhomogeneous environments, *Phys. Rev. E* **96**, 032105 (2017).
- [23] M. M. Meerschaert and C. Tadjeran, Finite difference approximations for fractional advection-dispersion flow equations, *J. Comput. Appl. Math.* **172**, 65 (2004).
- [24] T. Srokowski, Fractional Fokker-Planck equation for Lévy flights in nonhomogeneous environments, *Phys. Rev. E* **79**, 040104(R) (2009).
- [25] M. G. Nezhadhighi, Scaling characteristics of one-dimensional fractional diffusion processes in the presence of power-law distributed random noise, *Phys. Rev. E* **96**, 022113 (2017).
- [26] B. Dybiec, E. Gudowska-Nowak, and I. M. Sokolov, Underdamped stochastic harmonic oscillator driven by Lévy noise, *Phys. Rev. E* **96**, 042118 (2017).
- [27] D. A. Kessler and S. Burov, Stochastic maps, continuous approximation, and stable distribution, *Phys. Rev. E* **96**, 042139 (2017).
- [28] E. Barkai, Fractional Fokker-Planck equation, solution, and application, *Phys. Rev. E* **63**, 046118 (2001).
- [29] V. V. Yanovsky, A. V. Chechkin, D. Schertzer, and A. V. Tur, Lévy anomalous diffusion and fractional Fokker-Planck equation, *Physica A* **282**, 13 (2000).
- [30] C. Fernandez and M. F. J. Steel, On Bayesian modeling of fat tails and skewness, *J. Am. Stat. Assoc.* **93**, 359 (1998).
- [31] W. Feller, *An Introduction to Probability Theory and its Applications* (Wiley, New York, 1950), Vol. 2.
- [32] E. W. Montroll and J. T. Bendler, On Lévy (or stable) distributions and the Williams-Watts model of dielectric relaxation, *J. Stat. Phys.* **34**, 129 (1984).
- [33] V. M. Zolotarev, *One-Dimensional Stable Distributions* (American Mathematical Society, Providence, 1986).
- [34] R. N. Mantegna, Fast, accurate algorithm for numerical simulation of Lévy stable stochastic processes, *Phys. Rev. E* **49**, 4677 (1994).
- [35] J. Nolan, *Stable Distributions: Models for Heavy-Tailed Data* (Birkhauser, New York, 2003).
- [36] W. Feller, *An Introduction to Probability Theory and its Applications* (Wiley, New York, 1950), Vol. 2.
- [37] N. F. Johnson, P. Jefferies, and P. M. Hui, *Financial Market Complexity* (Oxford University, Oxford, 2003).
- [38] J. P. Nolan, Maximum likelihood estimation and diagnostics for stable distributions, in *Levy Processes: Theory and Applications* (Birkhäuser-Springer, Boston, 2001), pp. 379–400.
- [39] J. P. Nolan, Multivariate elliptically contoured stable distributions: Theory and estimation, *Computational Statistics* **28**, 2067 (2013).
- [40] Y. Liang and W. Chen, A survey on computing Lévy stable distributions and a new MATLAB toolbox, *Signal Processing* **93**, 242 (2013).
- [41] J. P. Nolan, Modeling financial data with stable distributions, in *Handbook of Heavy Tailed Distributions in Finance, Handbooks in Finance Vol. 1* (Elsevier, North-Holland, 2003), pp. 105–130.
- [42] R. N. Mantegna and H. E. Stanley, Stochastic Process with Ultraslow Convergence to a Gaussian: The Truncated Lévy Flight, *Phys. Rev. Lett.* **73**, 2946 (1994).
- [43] I. Koponen, Analytic approach to the problem of convergence of truncated Lévy flights towards the Gaussian stochastic process, *Phys. Rev. E* **52**, 1197 (1995).
- [44] G. L. Vasconcelos, A guided walk down wall street: An introduction to econophysics, *Braz. J. Phys.* **34**, 1039 (2004).
- [45] B. Podobnik, K. Matia, A. Chessa, P. Ch. Ivanov, Y. Lee, and H. E. Stanley, Time evolution of stochastic processes with correlations in the variance: Stability in power-law tails of distributions, *Physica A* **300**, 300 (2001).
- [46] B.-N. Huang, Do Asian stock market prices follow random walks? Evidence from the variance ratio test, *Applied Financial Economics* **5**, 251 (1995).
- [47] C. F. Lee, Gong-meng Chen, and O. M. Rui, Stock returns and volatility on China's stock markets, *Journal of Financial Research* **24**, 523 (2001).
- [48] B. V. Gnedenko and A. N. Kolmogorov, *Limit Distributions for Sums of Independent Random Variables* (Addison-Wesley, Reading, MA, 1954).
- [49] L. Breiman, *Probability* (Addison-Wesley, Reading, MA, 1968).
- [50] B. Mandelbrot, The variation of certain speculative prices, *The Journal of Business* **36**, 394 (1963).
- [51] V. V. Uchaikin and V. M. Zolotarev, *Chance and Stability: Stable Distributions and their Applications* (De Gruyter, Berlin, 2011).
- [52] D. Applebaum, *Lévy Processes and Stochastic Calculus* (Cambridge University, New York, 2009).
- [53] J. Bertoin, *Lévy Processes* (Cambridge University, New York, 1996).
- [54] S. M. Samuels, Positive integer valued infinitely divisible distributions, *Division of Mathematical Sciences* **406**, 1 (1975).
- [55] A. Klenke, Infinitely divisible distributions, in *Probability Theory* (Springer, New York, 2014), pp. 331–349.
- [56] G. Samorodnitsky and M. S. Taqqu, *Stable Non-Gaussian Random Processes: Stochastic Models with Infinite Variance* (Routledge, New York, London, 1994).

- [57] B. C. Arnold and D. L. Isaacson, On normal characterizations by the distribution of linear forms, assuming finite variance, *Stochastic Processes and their Applications* **7**, 227 (1978).
- [58] E. W. Weisstein, *CRC Concise Encyclopedia of Mathematics* (CRC, Boca Raton, FL, 1999).
- [59] M. Feldman, Hilbert transform in vibration analysis, *Mechanical Systems and Signal Processing* **25**, 735 (2011).
- [60] W. Gander and W. Gautschi, Adaptive quadrature—revisited, *BIT Numerical Mathematics* **40**, 84 (2000).
- [61] K. Yoneda, Riemann-Lebesgue theorem, *Analysis Mathematica* **7**, 297 (1981).
- [62] R. G. Bartle, Return to the Riemann integral, *Am. Math. Mon.* **103**, 625 (1996).
- [63] M. Abramowitz and I. A. Stegun, *Handbook of Mathematical Functions with Formulas, Graphs, and Mathematical Tables* (Dover, New York, 1965).
- [64] A. R. DiDonato and A. H. Morris, Jr., Computation of the incomplete gamma function ratios and their inverse, *ACM Transactions on Mathematical Software* **12**, 377 (1986).
- [65] R. Barakat, Evaluation of the incomplete gamma function of imaginary argument by Chebyshev polynomials, in *Mathematics of Computation* (JSTOR (Journal Storage), United States, 1961), pp. 7–11.
- [66] J. W. Pearson, *Computation of Hypergeometric Functions*, PhD. thesis, University of Oxford, 2009.
- [67] C. M. Bender and S. A. Orszag, *Advanced Mathematical Methods for Scientists and Engineers* (Springer, New York, 1999).
- [68] H.-G. Roos, M. Stynes, and L. Tobiska, *Robust Numerical Methods for Singularly Perturbed Differential Equations: Convection-Diffusion-Reaction and Flow Problems*, Springer Series in Computational Mathematics Vol. 24 (Springer, New York, 2008).
- [69] M. H. Holmes, *Introduction to Perturbation Methods*, Texts in Applied Mathematics Vol. 20 (Springer, New York, 2012).